Lafia Journal of Scientific & Industrial Research (LJSIR), Vol. 4(1), 2026
p-ISSN: 3026 – 9288 e-ISSN: 3027 – 1800 pages: 93 – 101
https://lafiascijournals.org.ng/index.php/ljsir/index ⇒ Published by the Faculty of Science,
Federal University of Lafia, Nasarawa State, Nigeria

Delineation of Lithology-based Radiogenic Heat Production from the Analysis of Airborne Radiometric Data of Azara and Environs, North-Central Nigeria

Sunday Ogayi Egede[1], Oke Israel Okwokwo[2], John Mathew Sawuta[3], Fidelis Iorzua Kwaghhua[4]*, Adegoke Blessing Adekemi[1] & Taiwo Adewumi[1]
[1]Department of Physics, Federal University of Lafia, Nigeria
[2]Department of Physics, University of Abuja, FCT, Nigeria
[3]National Space Research and Development Agency, NASRDA, Abuja, Nigeria
[4]Department of Geophysics, Federal University of Technology, Minna, Nigeria

Abstract

This study offers new insights into naturally occurring radioactive minerals in the Azara area and its environs, focusing on their impact on radiogenic heat production (RHP) for exploration geothermal energy. The radiometric data were analysed in relation to the lithology of the study area to determine the contribution of each lithologic unit to the estimated RHP. The study assessed radioelement concentrations, spatial distributions, and statistical summaries for each lithologic unit. Using radiometric data, the study mapped and analysed the spatial occurrence of potassium (K), thorium (eTh), and uranium (eU). The results show average concentrations of 1.23 % for K, 12.15 ppm for eTh, and 3.38 ppm for eU. Compared with crustal averages, K levels were lower, while eTh and eU levels were slightly higher. Radioelement abundance varied across rock types, with the highest concentrations in shales, siltstones, and sandstones. Estimated RHP values ranged from 0.90 to 2.70 μWm^{-3}, with an average of 1.70 μWm^{-3}. The estimated RHP value falls within the typical crustal range but is below the 4.0 μWm^{-3} threshold for a viable geothermal energy source.

Keywords: Geothermal energy, lithology, radioelement, radiometric data, radiogenic heat production

Article History

Submitted
December 28, 2025

Revised
February 27, 2026

First Published Online
March 04, 2026

Correspondences
F. I. Kwaghhua ✉
fidelisik@gmail.com

doi.org/10.62050/ljsir2026.v4n1.755

Introduction

A radiometric survey is conducted to measure the radiation components released to Earth's surface during radioactive decay. A spectrometer mounted on an aircraft detects the gamma rays emitted by decaying elements in the near-surface crust [1 – 4]. The acquired radiometric data can usually be analysed to support various target objectives, mostly subcrustal imaging and characterisation. An important deduction from radiometric data is the quantification of geo-energy generated during decay of radioactive elements in the near-subsurface [5 – 9].

Geothermal energy is the heat produced in the Earth's crust and core, via naturally occurring internal processes. Radiogenic heat is a major contributor to geothermal energy, where the crustal temperature gradient is built up by the continuous and spontaneous disintegration of radioactive elements [10, 11]. The level of geothermal energy generated in the crust is relatively dependent on the underlying lithological formations. This is because different lithologies have varying affinities for radioactive elements. However, amongst various geo-formations, granite in the basement complex and shale in the sedimentary formations have been linked with major sources of naturally occurring radioactive elements. A perspective on lithology-specific contributions to radiogenic heat is important, as it will provide a standard for subsequently mapping the geological formations of high-geothermal prospects [12 – 15].

The internal process that occurs in radioactive elements, releasing energy, is called radioactivity. It is the spontaneous disintegration of atomic nuclei, a feat that directly relates to the energy released. Atoms found in nature are either stable or unstable. An atom is stable if the forces between the particles in the nucleus are balanced. An atom is unstable (radionuclide) if these forces are unbalanced, that is, if the nucleus has an excess of internal energy. The unstable atoms are called radionuclides [16 – 19]. The instability of an atomic nucleus may result from an excess of either neutrons or protons; therefore, radioactivity is a result of an atom attempting to reach stability by ejecting nucleons (neutrons or protons), forming new elements, and releasing energy in other forms. Sometimes this new element formed may be unstable; the process is repeated until a stable element is formed. The series of transformations that a radionuclide undergoes to reach stability is called a decay chain. The energy released

during radioactive decay is called radiation, which exists in three forms (alpha, beta, and gamma radiation) [20 – 21].

In this study, radiogenic heat production will be evaluated from gamma-ray emission from K, eTh, and eU. The study will outline the geological formations of the Azara environs, the radioactive element compositions, and the potential radioactivity that could be explored for geothermal exploration.

Materials and Methods

Location and geologic setting of the study area

The study area is Azara, located in Awe LGA in the South-Eastern part of Nasarawa State, North Central Nigeria. The area lies approximately between latitudes 8° 21′ 43 N and 8° 19′ 22 N, and longitudes 9° 14′ 48'' E and 9° 18′ 25'' E, and it covers a land mass of approximately 2529 km^2 (Fig. 1). it can be accessed via roads, rivers, and networks of footpaths. The town's main commercial activities are farming and mining [22].

Geologically, the study area lies within the Middle Benue Trough, a rift basin located in central West Africa, extending approximately 800 km in a NNE–SSE direction and spanning about 150 km in width. Its southern boundary aligns with the northern edge of the Niger Delta, while its northern boundary meets the southern limit of the Chad Basin. The trough holds up to 6,000 meters of Cretaceous to Tertiary sediments, with those predating the mid-Santonian period experiencing significant compression, folding, faulting, and uplift in various areas [23].

The stratigraphic succession of the Middle Benue Trough, particularly in the Obi/Lafia area, consists of six Upper Cretaceous lithogenic formations. These include the Albian-aged Arufu, Uomba, and Gboko Formations, collectively known as the Asu River Group [24]. Overlying these are the Cenomanian–Turonian Keana and Awe Formations, followed by the Cenomanian–Turonian Ezeaku Formation, which corresponds to the Konshisha River Group and the Wadata Limestone in the Makurdi area. The Late Turonian–Early Santonian Awgu Formation, which contains coal deposits, lies conformably atop the Ezeaku Formation. In the Makurdi area, the Makurdi Sandstone inter-fingers with the Awgu Formation. The mid-Santonian period was marked by folding throughout the Benue Trough. Subsequently, the post-folding Campano-Maastrichtian Lafia Formation marked the final phase of sedimentation in the Middle Benue Trough, after which extensive volcanic activity dominated the region during the Tertiary period. The study area is made up of two lithologic units, including an alluvium deposit in the southwestern part and sandstone belonging to the Eze Aku group in the northern and southeastern parts of the study area (Fig. 2).

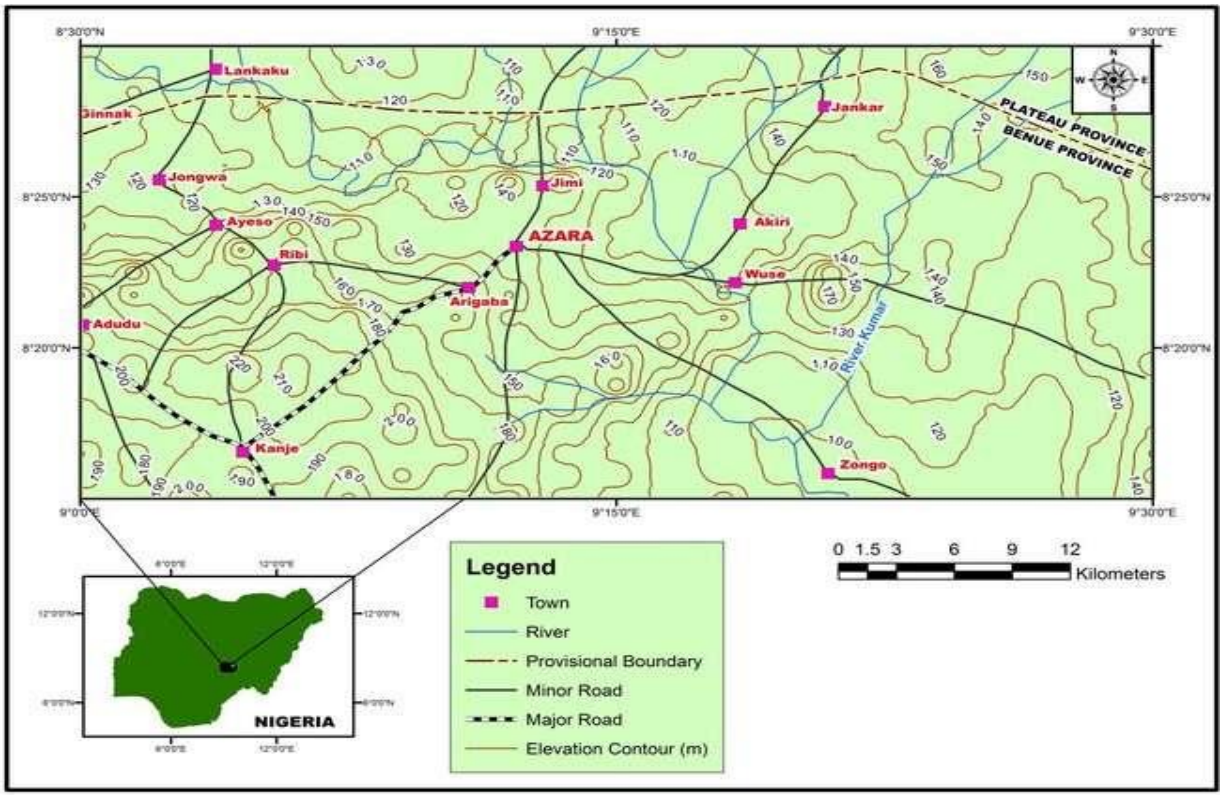

Figure 1: Location map of the study area [23]

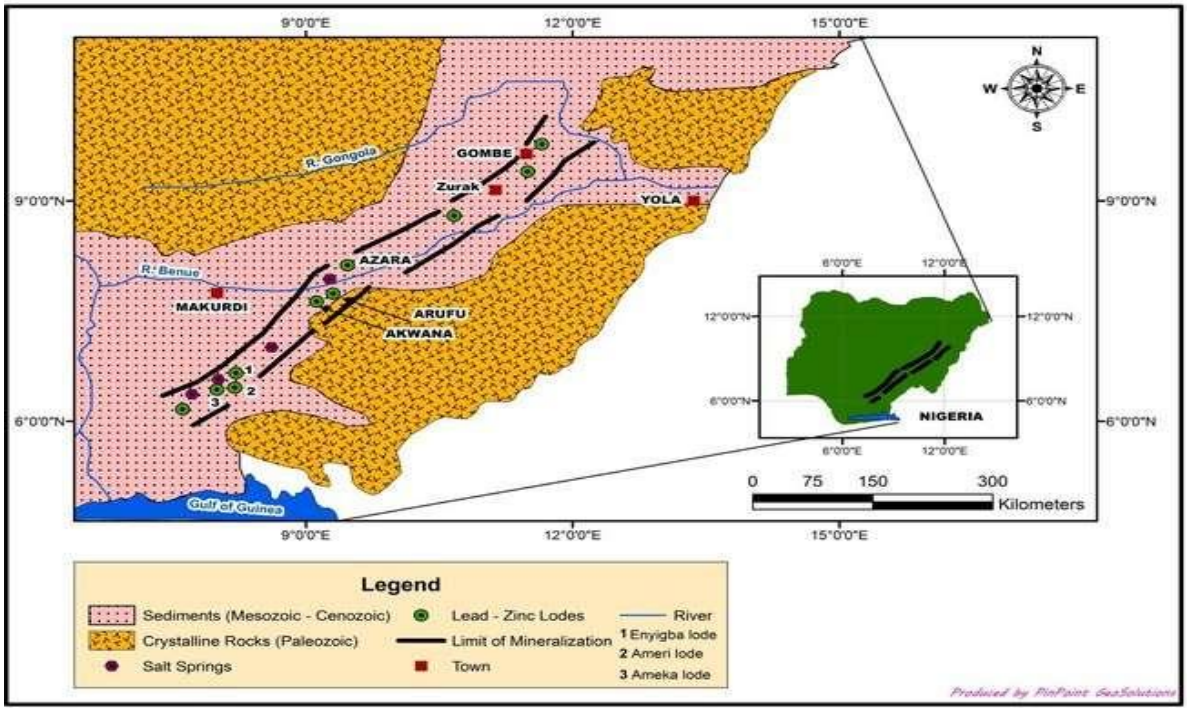

Figure 2: Geological map of the study area [23]

Airborne gamma-ray spectrometry data (AGRS) source

The AGRS dataset used for this study was procured from the Nigerian Geological Survey Agency (NGSA). The airborne geophysical survey was carried out between the years 2005 and 2009 by Fugro Airborne Survey on behalf of the Nigerian Geological Survey Agency. AGRS datasets were collected using GR-820-3 with radiometric crystal GPX 1024/256. This airborne geophysical data was collected at an interval of 0.1 sec at an altitude of 100 m along a flight line spacing of 500 m in NW-SE, with a sensor mean terrain clearance of 80 m, a tie line spacing of 2 km, and a flight line trend of 125 degrees. For a half-degree sheet, the maps were created on a scale of 1:100,000. The acquisition agency had also processed the GRS datasets to correct for background radiation arising from cosmic rays and aircraft anomalies caused by altitude changes relative to the ground. The corrected data provided the exact measured elemental concentrations of K, eU, and eTh.

Radioactive heat production rate (RHPR)

Radioactive heat production is the rate at which heat is generated in a material due to the radioactive decay of unstable nuclei. The most common radioactive isotopes that contribute to radiation heat production are 238^{U}, 232^{Th} and 40^{K}. Radiation heat production from naturally occurring radioactive material is hazardous in industries such as mining and oil production. It is measured in watts per cubic meter (W/m^3) [25 – 26]. This is obtained using equation (1) below.

$$RHP(\mu Wm^{-3}) = 10^{-5}\,\rho\,(3.48CA_K + 9.52CA_U + 2.56CA_{Th}) \quad (1)$$

where RHPR is radioactive heat production rate expressed in μWm^{-3}, ρ is the sample density in kgm^{-3}, C_{AU}, and C_{ATh} are the uranium and thorium concentration in ppm, and C_{AK} is the total potassium concentration in %

Results and Discussion

The analysis and results of this study have comprehensively synthesized evaluations and estimates of radiogenic heat production (RHP). The analysis focused on the host lithologies been source of the radioactive decay generating energy that is disseminated into the environment.

Lithology based occurrence of natural radioactive elements (K, eTh, eU) within Wamba environs

The main radioactive elements mapped in this study were those within the detectable range of gamma-spectroscopic surveys. The concentrations of Potassium (K) measured as a percentage (%), equivalent Thorium (eTh), and Uranium (eU) in parts per million (ppm) were computed as gridded images in Fig. 3a—c, respectively. The maps were produced with colours visually connoting the concentration values of the radioelements. High concentration areas (HC) correspond to red to pink colours, moderate concentrations (MC) to green to yellow colours, and low concentrations (LC) to blue colours. Table 1 presents the statistical summary of the estimated concentration of the radio elements (K%, eTh, and eU) within the study area.

A spatial inspection of Potassium occurrence within the Azara environs is mapped in Fig. 3a. Quantitatively, the range of potassium concentration with Azara varied from 0.53 to 3.45 %. The red and pink colours depicting high concentrations (HC) are mapped and enclosed within black dotted lines. High potassium signatures are observed at the southeastern region, extending partly to southwest and northeast, also at the western edge. While low concentrations (LC) are mapped in blue colours and enclosed within white dotted lines, moderate concentrations are mapped in

green and yellow. The low concentrations are prominent in the northwestern regions, while the moderate concentrations trend from the southwest to the northeast, captured between LC and HC. Lithologically, both high and low potassium concentrations are mapped within the regions occupied by sandstones and alluvium.

The equivalent Thorium (eTh) (Fig. 3b) within the Azara regions showed high concentrations (HC) in the northern and southwestern regions, depicted in red and pink, respectively. The main high-concentration (HC) areas are enclosed in black dotted lines, while the low-concentration (LC) areas are enclosed in dotted lines, mainly in the south-eastern region. The moderate concentrations, shown in yellow and green, are mainly mapped in the central regions of Azara. Peak concentrations in pink colours were mapped largely within the sandstone of the Eze Aku group, while the southwestern regions, which host both moderate and high concentrations, are partly dominated by alluvium and black shale mixed with siltstones. On average, the value of equivalent thorium concentration ranges from 3.96 to 19.33 ppm.

The spatial distribution of Equivalent Uranium concentrations within the study area is captured in Fig. 3c. High concentrations (HC) in red colours are generally observed in the northern and southwestern regions. Moderate concentrations (MC) are captured in the north-eastern regions in yellow and green colours, while low concentrations (LC) are mapped in blue colours at the south-eastern edge. HC are enclosed with black dotted lines while LC are within white dotted lines, and MC are observed in between HC and LC. Numerical values of equivalent uranium range from 1.15 to 5.84 ppm. The prominent litho-unit mapped with high eU in the upper northern regions is mainly sandstone of the Eze Aku group.

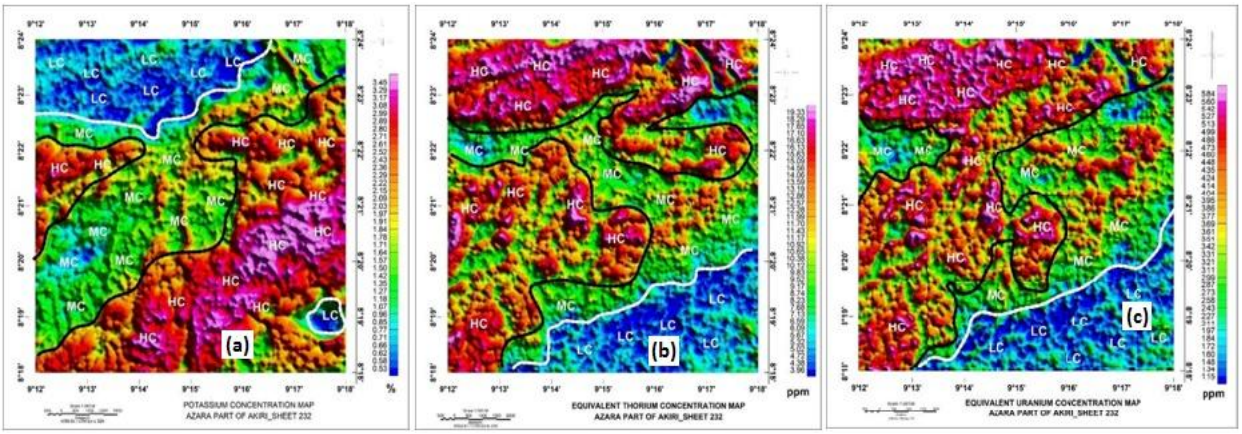

Figure 3: Concentration maps of the study area (a) K% (b) eTh (c) eU

Table 1: Statistical estimate of elemental concentrations of K, eTh and eU within study area

S/N	Lon	Lat	Rock ID	Rock Type	K(%)				eTh(ppm)				eU(ppm)			
					Min	Max	Av	SD	Min	Max	Av	SD	Min	Max	Av	SD
1	9.237	8.342	Al1	Alluvium	0.60	3.40	2.00	0.80	1.90	19.10	9.70	3.90	0.80	5.10	3.10	1.20
2	9.233	8.339	Al2		0.80	3.40	2.20	0.70	2.90	18.70	9.10	3.60	0.50	5.80	3.00	1.20
3	9.228	8.336	Al3		0.80	3.30	2.10	0.70	4.00	19.90	10.50	3.80	0.70	7.90	3.50	1.40
4	9.232	8.341	Al4		0.60	3.30	2.00	0.70	3.80	18.70	9.80	3.70	1.00	5.50	3.20	1.20
5	9.236	8.334	Al5		1.00	3.60	2.30	0.70	3.30	18.00	9.70	3.60	1.00	6.60	3.20	1.30
6	9.217	8.328	Esh1	Black shale, Siltstone and Sandstone	0.70	3.30	1.60	0.70	6.30	20.00	12.30	2.70	2.60	5.50	3.90	0.80
7	9.215	8.319	Esh2		0.80	2.30	1.50	0.50	6.90	15.30	11.40	1.90	2.60	5.10	3.70	0.60
8	9.207	8.319	Esh3		0.70	1.80	1.20	0.20	8.40	17.90	13.90	2.20	3.40	5.60	4.40	0.60
9	9.220	8.312	Esh4		1.80	2.90	2.50	0.40	10.30	16.70	13.40	1.70	3.10	5.40	4.30	0.60
10	9.204	8.320	Esh5		1.00	1.60	1.30	0.20	9.00	19.20	13.10	2.80	3.00	5.50	4.20	0.80
11	9.293	8.392	Ess1	Sandstones	0.90	1.80	1.30	0.20	8.20	20.80	17.20	3.00	1.90	5.50	4.50	0.90
112	9.283	8.381	Ess2		0.20	2.80	1.60	0.70	1.90	20.90	12.40	5.30	0.10	6.50	3.60	1.50
13	9.268	8.368	Ess3		0.50	3.70	2.10	1.00	5.70	22.30	12.30	3.50	1.40	6.50	3.90	1.10
14	9.254	8.353	Ess4		0.40	3.80	1.60	1.00	3.70	18.70	11.20	4.40	0.90	6.50	3.70	1.40
15	9.230	8.390	Ess5		0.50	1.00	0.80	0.10	16.40	23.30	18.90	1.80	5.20	6.80	5.90	0.40
16	9.254	8.383	Ess6		0.50	2.00	0.70	0.30	7.20	19.40	11.10	2.50	1.70	6.30	3.80	0.80
17	9.273	8.368	Ess7		1.20	3.10	2.00	0.50	4.10	14.10	8.90	2.80	1.00	4.20	2.80	0.80
18	9.277	8.350	Ess8		1.80	3.30	2.50	0.40	9.30	15.00	12.10	1.20	2.80	5.10	3.80	0.50
19	9.282	8.331	Ess9		2.90	3.60	3.20	0.20	3.54	7.50	5.80	1.20	0.60	2.90	1.60	0.50
20	9.290	8.318	Ess10		0.60	2.30	1.20	0.50	3.90	6.40	5.20	0.60	1.20	2.40	1.80	0.40

Lithological base evaluation of radioelements concentrations

Three lithological units (Alluvium – Al, Black shale, silt and sandstone – Esh, and sandstones – Ess) were mapped and examined for radiogenic elements composition. Minimal, maximal, average, and standard deviation values were evaluated for each radioelement (K, eTh, and eU) as presented in Table 1. Each litho—unit showed distinct average compositions as follows: Potassium: (Al: 2.0 – 2.30 %); (Esh: 1.20 – 2.50 %); (Ess: 0.70 – 3.20 %), Equivalent thorium: (Al: 9.10 – 10.50 ppm); (Esh: 11.40 – 13.90 ppm); (Ess: 5.20 – 18.90 ppm), Equivalent uranium: (Al: 3.10 – 3.50 ppm); (Esh: 3.70 – 4.40 ppm); (Ess: 1.60 – 5.90 ppm). Apparently, higher K, eTh, and eU are estimated in the sandstones – Ess.

Estimation of radiogenic heat production

The radiogenic production capacity of radioactive elements within Azara was estimated utilising the empirical formula stated in equation 1. The quantity of heat production was estimated for each radioactive element, QK, QeTh, and QeU, to measure the individual element's contribution to the composite radiogenic heat production (RHP) of Azara environs. Heat production due to potassium ranged from 0.06 to 0.28 μWm^{-3}, with an average of 0.16 μWm^{-3}. The quantity of heat from equivalent thorium varied from 0.33 to 1.21 μWm^{-3}, with an average of 0.78 μWm^{-3}. Heat production from equivalent uranium varied from 0.38 to 1.40 μWm^{-3}, with an average of 0.86 μWm^{-3}. The combined heat production value, taking into account the contributions of the three elements, varied from 0.9 to 2.70 μWm^{-3}, with an average of 1.70 μWm^{-3} (Table 2).

Table 2: Estimates of radiogenic heat production

Lon	Lat	Rock ID	K (%)	eTh ppm	eU ppm	Qk	QeTh	QeU	RHP μWm^{-3}
9.237	8.342	Al1	2.00	9.70	3.10	0.17	0.62	0.74	1.53
9.233	8.339	Al2	2.20	9.10	3.00	0.19	0.58	0.71	1.49
9.228	8.336	Al3	2.10	10.50	3.50	0.18	0.67	0.83	1.69
9.232	8.341	Al4	2.00	9.80	3.20	0.17	0.63	0.76	1.56
9.236	8.334	Al5	2.30	9.70	3.20	0.20	0.62	0.76	1.58
9.217	8.328	Esh1	1.60	12.30	3.90	0.14	0.79	0.93	1.85
9.215	8.319	Esh2	1.50	11.40	3.70	0.13	0.73	0.88	1.74
9.207	8.319	Esh3	1.20	13.90	4.40	0.10	0.89	1.05	2.04
9.22	8.312	Esh4	2.50	13.40	4.30	0.22	0.86	1.02	2.10
9.204	8.32	Esh5	1.30	13.10	4.20	0.11	0.84	1.00	1.95
9.293	8.392	Ess1	1.30	17.20	4.50	0.11	1.10	1.07	2.28
9.283	8.381	Ess2	1.60	12.40	3.60	0.14	0.79	0.86	1.79
9.268	8.368	Ess3	2.10	12.30	3.90	0.18	0.79	0.93	1.90
9.254	8.353	Ess4	1.60	11.20	3.70	0.14	0.72	0.88	1.74
9.23	8.39	Ess5	0.80	18.90	5.90	0.07	1.21	1.40	2.68
9.254	8.383	Ess6	0.70	11.10	3.80	0.06	0.71	0.90	1.68
9.273	8.368	Ess7	2.00	8.90	2.80	0.17	0.57	0.67	1.41
9.277	8.35	Ess8	2.50	12.10	3.80	0.22	0.77	0.90	1.90
9.282	8.331	Ess9	3.20	5.80	1.60	0.28	0.37	0.38	1.03
9.29	8.318	Ess10	1.20	5.20	1.80	0.10	0.33	0.43	0.87
Minimum Value			**0.70**	**5.20**	**1.60**	**0.06**	**0.33**	**0.38**	**0.90**
Maximum Value			**3.20**	**18.90**	**5.90**	**0.28**	**1.21**	**1.40**	**2.70**
Mean Value			**1.79**	**11.40**	**3.60**	**0.16**	**0.73**	**0.86**	**1.70**

The mapping of radioactive elements in the Azara study area revealed significant patterns in spatial distribution and concentration. The three major litho-units mapped within the study area (Esh, Al, and Ess) are classified as sedimentary units with varying lithofacies. The lithologies (Esh – Black Shale and Siltstone, Al – Alluvium, and Ess – Sandstone) showed distinct levels of radioactive element composition. The elements' trend of occurrence showed higher concentrations of potassium in black shale and sandstones than in alluvium, and the same was observed for Equivalent thorium and uranium. The radioactive element's occurrence affirms the fact that black shale comprises heavy minerals such as garnet and monazite which are good hosts for thorium and uranium [27 – 29].

Statistically generated average concentrations of elements (K, eTh and eU) were in the range of continental crustal mean values.

For elemental concentration, the average value of 1.79 % for Potassium slightly falls below the crustal average of 2.0 – 2.5 %. The equivalent thorium estimated average value of 11.40 ppm was within the crustal average range of 8 – 12 ppm. The equivalent uranium estimated average of 3.60 ppm was slightly above the crustal average range of 2.0 – 3.0 ppm.

The average heat production of the three radioactive elements was estimated as 0.16, 0.73, and 0.86 μWm^{-3}, for QK, QeTh, and QeU, respectively. The combined heat production from K, eTh, and eU was estimated at 1.70, and the RHP value falls below the known continental and crustal average of 2.0–2.95 μWm^{-3}, [13, 30]. Fig. 4 depicts the trend in radiogenic heat production in the Azara area. High heat production regions above 2.0 μWm^{-3} are marked as (HHP), moderate heat production (MHP) and low heat production as (LHP). Despite the general spatial spread averaging 1.70 μWm^{-3}, values above 2.5 μWm^{-3}, dominate the upper northern regions, with pockets in the central regions. High concentrations of eTh and eU in the designated north and central regions produced more heat than the high concentration of potassium at the south-eastern end. The variation in heat production reflects the element's relative abundance and varying energy production during radioactive decay, with potassium showing the least capacity [10, 31, 32].

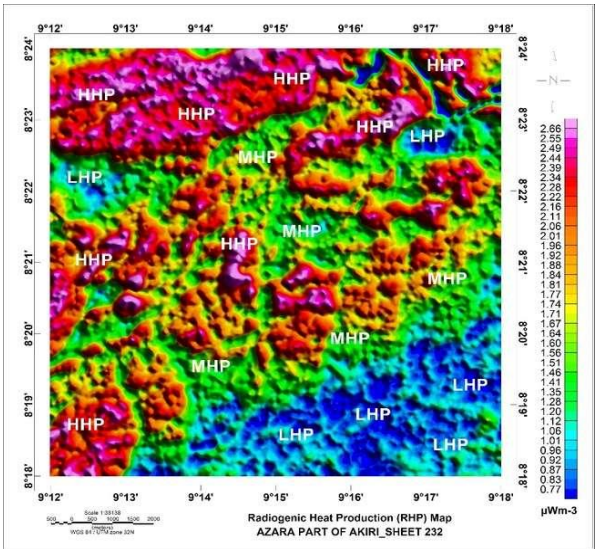

Figure 4: Radiogenic heat production map of study area

Graphical bar plots visualising variation in element concentrations, radiogenic heat production of individual elements and composite radiogenic heat production are presented in Fig. 5a—c, respectively.

Host capacities of litho-units for radioelements show minimal (0.70 %) and maximal (3.20 %) potassium values within the sandstones (Ess). This heterogeneity can be linked to potassium minerals' susceptibility to leaching during weathering [33]. Equivalent thorium is portrayed as relatively more abundant due to its nature of resistance to leaching. eTh is significantly present in every litho-unit and dominant in the sandstones (Ess). Equivalent uranium is captured in the three litho-units with higher values exceeding the crustal average of 3.0 ppm within the shales and sandstones.

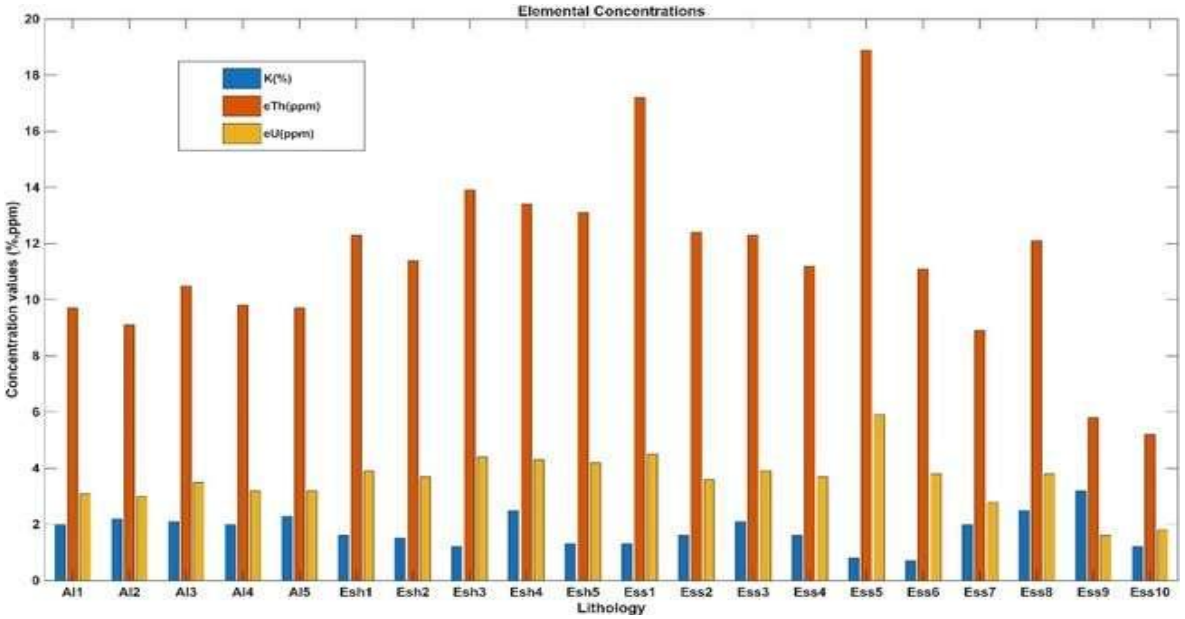

Figure 5a: Element concentrations and lithological units plot

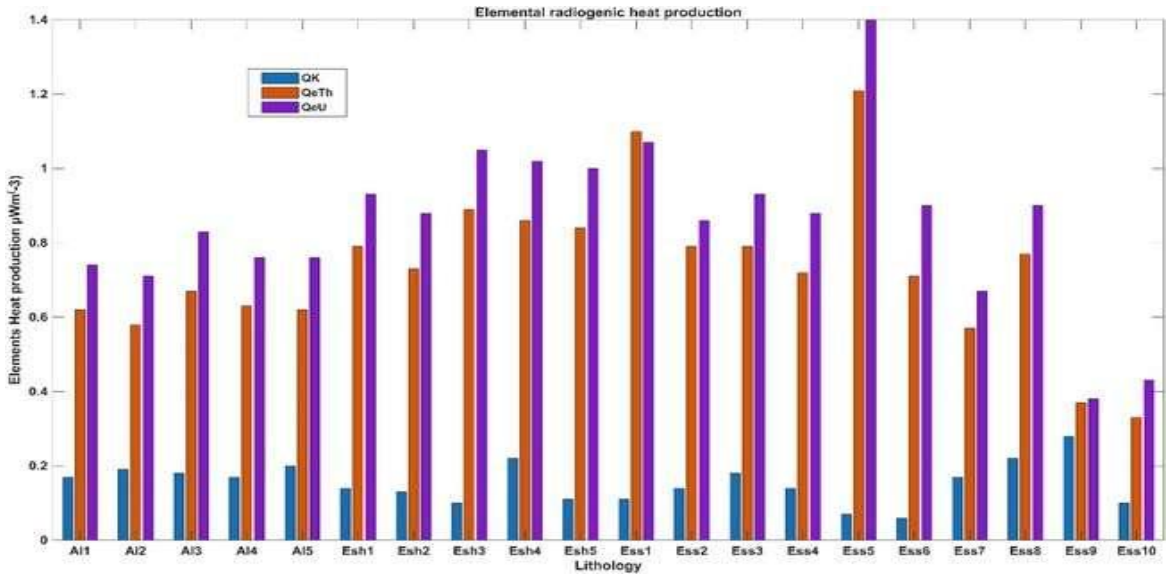

Figure 5b: Elements radiogenic heat production and lithological units plot

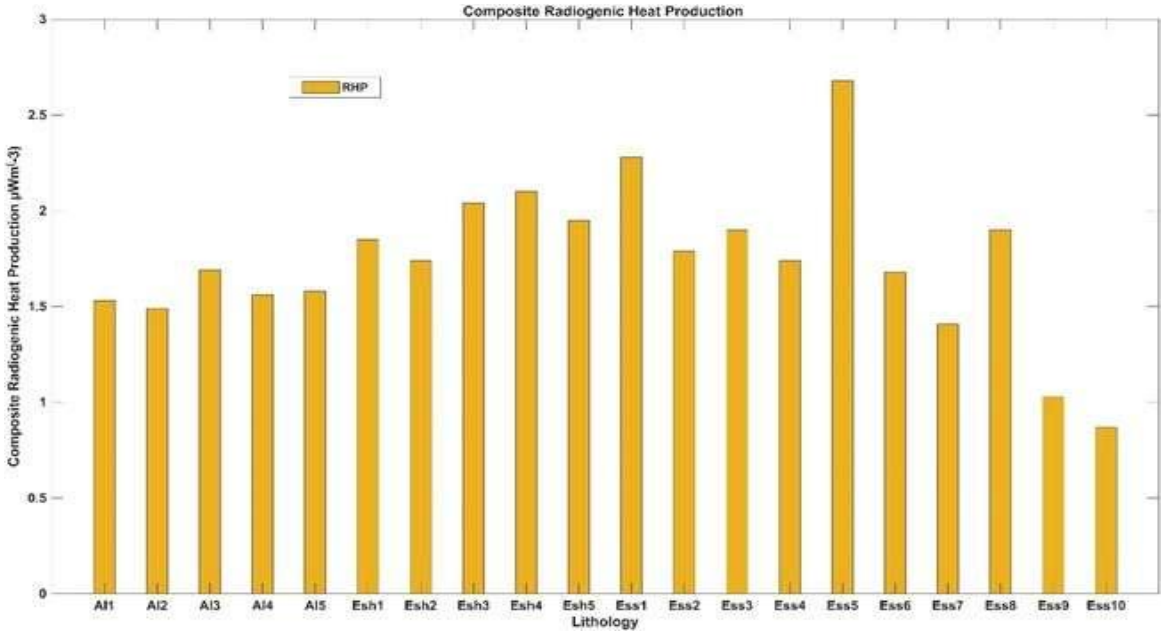

Figure 5c: Composite radiogenic heat production and lithological units plot

The heat production capacities per element and relative to lithological units are presented in Fig. 5b, while the composite heat production due to the three radiogenic elements is presented in Fig. 5c. The bar plots generally showed that uranium was the major contributor to heat production, followed by thorium, with potassium contributing the least [31, 34, 10]. While peak and low heat production were recorded within the sandstones (Ess), a record of steadily high heat production is observed within the shale and siltstones litho-unit. Shales are generally associated with high heat production within the sediments [35, 36]. Imperatively, the regions of shale (Esh) and alluvium (Al) within the study area will be more viable sources of radiogenic heat despite spikes of anomalous values within the sandstones (Ess).

Conclusion

The study mapped the relative concentrations and spatial distribution of radioactive elements (K, eTh, and eU) within the capture range of a gamma-ray spectrometric survey. A lithology-based measure of the radioactive elements was carried out to map their relative abundance and occurrence, and to identify their sources and host rock types. Three lithologies (rock types) were identified and mapped in the Azara area: Alluvium (Al), Black shale and Siltstone (Esh), and Sandstone of the Eze Aku Group.

The lithology-based assessment of radioactive elements and corresponding heat production revealed significant heat production across the three mapped lithologies (Al, Esh, and Ess). High RHP values above 2.5 μWm^{-3} dominate the upper northern regions, with pocket traces in the central regions, which also represent areas of interest for radiogenic heat sources within the Aazra environs. The peak value of 2.70 μWm^{-3} recorded at the north-western regions of the study area is insufficient compared to 4.0 μWm^{-3} recommended for a good geothermal source. However, the designated high-RHP region can be explored for other, less demanding industrial heating requirements.

Conflict of interest: The authors declare no conflict of interest.

References

[1] Abbady, A. G. (2010). Evaluation of heat generation by radioactive decay of sedimentary rocks in Eastern Desert and Nile Valley, Egypt. *Applied Radiation and Isotopes*, 68(10), 2020-2024.

[2] Aisabokhae, J. & Adeoye, M. (2020). Spatial distribution of radiogenic heat in the Iullemmeden basin–Precambrian basement transition zone, NW Nigeria. *Geology, Geophysics and Environment*, 46(3), 239-250.

[3] Faweya, E. B., Agbetuyi, O. A., Talabi, A. O., Adewumi, T. & Faweya, O. (2021). Radiological Implication of 222 Rn concentrations in waters from quarries environs, correlation with 226 Ra concentrations and rocks geochemistry. *Arabian Journal of Geosciences*, 14, 1-15.

[4] Reinhardt, N. & Herrmann, L. (2019). Gamma-ray spectrometry as versatile tool in soil science: A critical review. *Journal of Plant Nutrition and Soil Science*, 182(1), 9-27.

[5] Megwara, J. U., Udensi, E. E., Olasehinde, P. I., Daniyan, M. A. & Lawal, K. M. (2013). Geothermal and radioactive heat studies of parts of southern Bida basin, Nigeria and the surrounding basement rocks. *Int. J. Basic Appl. Sci*., 2(1), 125-139.

[6] Sedara, S. O. & Ojoawo, A. I. (2018). Ground radiometric survey and geothermal energy investigation in Ikogosi Warm Spring, Ekiti,

Southwestern Nigeria. *Journal of Science Research*, 17(1), 53-61.

[7] Clauser, C. (2021). Radiogenic heat production of rocks. In *Encyclopedia of Solid Earth Geophysics* (pp. 1304-1310). Cham: Springer International Publishing.

[8] Adewumi, T., Salako, K. A., Akingboye, A. S., Muztaza, N. M., Alhassan, U. D. & Udensi, E. E. (2023). Reconstruction of the subsurface crustal and radiogenic heat models of the Bornu Basin, Nigeria, from multi-geophysical datasets: Implications for hydrocarbon prospecting. *Advances in Space Research*, 71(10), 4072-4090.

[9] Adetona Adebayo, A., Abdulwaheed Adewuyi, R., Aliyu Bukola, S., John M, K. & Kwaghhua I, F. (2024). Estimating the heat flow, Geothermal Gradient and Radiogenic Heat within the Young Granites of Jos Plateau North Central Nigeria. *Journal of Earth and Space Physics*, 49 (4), 69- 81

[10] McCay, A. T., Harley, T. L., Younger, P. L., Sanderson, D. C. & Cresswell, A. J. (2014). Gamma-ray spectrometry in geothermal exploration: State of the art techniques. *Energies*, 7(8), 4757-4780.

[11] Salako, K. A., Adetona, A. A., Alhassan, U. D., & Rafiu, A. A. (2020). Assessment of Geothermal Potential of Parts of Middle Benue Trough, North-East Nigeria.

[12] Akingboye, A. S., Ogunyele, A. C., Jimoh, A. T., Blessing, O., Adedapo, A., Adeola, O. & Ajayi, T. (2021). Radioactivity, radiogenic heat production and environmental radiation risk of the Basement Complex rocks of Akungba-Akoko, southwestern Nigeria : insights from in situ gamma-ray spectrometry. *Environmental Earth Sciences*, 1–24. https://doi.org/10.1007/s12665-021-09516-7

[13] Jaupart, C., & Mareschal, J. C. (2021). Radiogenic heat production in the continental crust. In *Encyclopedia of Solid Earth Geophysics* (pp. 1298-1303). Cham: Springer International Publishing.

[14] Faweya, E. B., Ayeni, M. J., Olowomofe, G. O. & Akande, H. T. (2018). Estimation of radiation exposure in soils and organic (animal) and inorganic (chemical) fertilizers using active technique. *International Journal of Environmental Science and Technology*, 15(9), 1967-1982.

[15] El Gendy, N. H., El Deen, T. M. S., Elkhodary, S. T., Sabra, M. E. M. & Youssef, M. A. S. (2024). Environmental impact assessment and determination of radiogenic heat production in the North Jabal Maghrabiyah area, Central Eastern Desert, Egypt. *Applied Radiation and Isotopes*, 211, 111398.

[16] IAEA (2003). Mapping using gamma ray. July.

[17] Bertulani, C. A. (2007). Nuclear Physics in a Nutshell.

[18] Lawson, R. (n.d.). An Introduction to Radioactivity by October 1999, 1–20.

[19] Kratz, J. V. (2022). *Nuclear and Radiochemistry: Fundamentals and Appl.*. John Wiley & Sons.

[20] Unit, I. (1967). Nuclear Structure.

[21] L'Annunziata, M. F. (Ed.). (2012). *Handbook of Radioactivity Analysis*. Academic press.

[22] Aliyu, U. S. A., Hamza, A. M., & Usman, A. M. (2019). Radiometric Evaluation of Radionuclides in Some Selected Mining Sites across Azara Development Area of Nasarawa State, Nigeria. *Journal of Science and Mathematics Letters*, 8(1), 27-36.

[23] Aladesanmi, A. O., Ogundana, A. K., Olowookere, A. A. & Jenakumo, L. (2018). Geological characterization of Azara barite mineralization, Middle Benue Trough Nigeria. *J. Environ Earth Sci.*, 8(3), 44-46.

[24] Offodile, M. E. (1984). The geology and tectonics of Awe brine field. *Journal of African Earth Sciences (1983)*, 2(3), 191-202.

[25] Rybach, L. (1976). Radioactive heat production in rocks and its relation to other petrophysical parameters. Pure and Applied Geophysics, 114, 309-317.

[26] Faweya, E. B., Olojede, D. S., Adewumi, T. & Ikubanni, S. O. (2023). Radiogeochemistry, mineralogy, lithology, radiogenic heat production, and health implication using airborne radiometric data of Ilesha and its surroundings. *Environmental Monitoring and Assessment*, 195(5). https://doi.org/10.1007/s10661-023-11168-y

[27] Abdel-Karim, A. A. M., Zaid, S. M., Moustafa, M. I. & Barakat, M. G. (2016). Mineralogy, chemistry and radioactivity of the heavy minerals in the black sands, along the northern coast of Egypt. *J. of Afri. Earth Sci.*, 123, 10-20.

[28] Fares, S. (2017). Measurements of natural radioactivity level in black sand and sediment samples of the Temsah Lake beach in Suez Canal region in Egypt. *Journal of Radiation Research and Applied Sci*, 10(3), 194-203.

[29] Alshahrani, B., Fares, S., Salman, M. & Korna, A. H. (2025). Assessment of natural radioactivity levels in black sand and sand sediments in the Mediterranean coast region, Egypt. *Environmental Challenges*, 18, 101061.

[30] Liao, D., Feng, D., Luo, J. & Yun, X. (2023). Relationship between radiogenic heat production in granitic rocks and emplacement age. *Energy Geoscience*, 4(4), 100157.

[31] Adewumi, T., Faweya, B. E., Abimbola, O. J., Zemnaan, Y. C., Mohammed, M. A. & Kwaghhua, F. I. (2025). Radiological hazard assessment and radiogenic heat production of Keffi and its environs: insight from the analysis of airborne gamma-ray spectrometry data. *Environmental Monitoring and Assessment*, 197(9), 995.

[32] Bajoga, A. D., Al-Dabbous, A. N., Abdullahi, A. S., Alazemi, N. A., Bachama, Y. D. & Alaswad, S. O. (2019). Evaluation of elemental concentrations of uranium, thorium and potassium in top soils from Kuwait. *Nuclear Engineering and Technology*, 51(6), 1638-1649.

[33] Liang, H., Yin, F., Zhang, J., Zhang, J., Zhao, Y., Zhao, T., ... & Wang, Z. (2025). Impacts of long-term drip irrigation on K-bearing mineral weathering and microbial potassium mobilization in arid cotton systems. *Agricultural Water Management*, 322, 110000.

[34] Orozova-Bekkevold, I. (2024). In-situ radiogenic heat production in the Cenozoic sediments of the North sea. *Physics and C*.

[35] Bakar Yusuf, A., San Lim, H. & Abir, I. A. (2023). Radiogenic heat production estimation towards sustainable energy drive in northeastern Nigeria. *Heliyon*, 9(6).

[36] Bubu, A. (2017). Radiogenic heat production due to natural radionuclides in the sediments of Bonny River, Nigeria. *Journal of Scientific Research and Reports*.

Citing this Article

Egede, S. O., Okwokwo, O. I., Sawuta, J. M., Kwaghhua, F. I., Adekemi, A. B., & Adewumi, T. (2026). Delineation of lithology-based radiogenic heat production from the analysis of airborne radiometric data of Azara and environs, North-Central Nigeria. *Lafia Journal of Scientific and Industrial Research, 4*(1), 93 – 101. https://doi.org/10.62050/ljsir2026.v4n1.755